Carbohydrate Polymers 204 (2019) 42–49

Contents lists available at ScienceDirect

Carbohydrate Polymers

journal homepage: www.elsevier.com/locate/carbpol

One-pot fabrication of durable antibacterial cotton fabric coated with silver nanoparticles via carboxymethyl chitosan as a binder and stabilizer

QingBo Xu[a], WeiShi Zheng[a], PanPan Duan[a], JiaNing Chen[b], YanYan Zhang[a], FeiYa Fu[a], HongYan Diao[b,*], XiangDong Liu[a,*]

[a] Key Laboratory of Advanced Textile Materials and Manufacturing Technology, Ministry of Education, College of Materials and Textile, Zhejiang Sci-Tech University, Xiasha Higher Education Zone, Hangzhou, 310018, China

[b] State Key Laboratory for Diagnosis and Treatment of Infectious Diseases, Collaborative Innovation Center for Diagnosis and Treatment of Infectious Diseases, The First Affiliated Hospital, College of Medicine, Zhejiang University, 310003, Hangzhou, China

ARTICLE INFO

Keywords:
One-pot preparation
Carboxymethyl chitosan
Silver nanoparticles
Antimicrobial cotton

ABSTRACT

In this article, durable antimicrobial cotton fabric was prepared by a one-pot modification process using a colloidal solution of silver nanoparticles (Ag NPs) stabilized by carboxymethyl chitosan (CMC). Due to coordination bonds between the amine groups of CMC and the Ag NPs and the ester bonds present between the carboxyl groups of CMC and the hydroxyl groups of cellulose, the Ag NPs were tightly immobilized onto the cotton fiber surface. As a result, the Ag NPs that were adhered on the cotton fabrics have uniform dispersion and small size, ranging from 10 nm to 80 nm. This provides the cotton fabric with remarkable and durable antibacterial activity against both *S. aureus* and *E. coli*. After 50 laundering cycles, the bacterial reduction rate (BR) for the modified cotton fabric remained over 94%. This method is simple, and it is particularly suitable for the industrial finishing process.

1. Introduction

Cotton fabric plays key roles in our daily life due to its excellent properties: it is comfortable, flexible, water-absorbing, and air-permeable. To expand cotton fabric applications, numerous modifications to enhance antimicrobial properties (Fei, Liu, Zhu, Wang, & Yu, 2018; Rauytanapanit, Opitakorn, Terashima, Waditee-Sirisattha, & Praneenararat, 2018; Salat et al., 2018), UV protection (Hu et al., 2018; Ren et al., 2018), fire resistance (Yang, Zhang, Fu, & Liu, 2017) and water repellence (Feng, Sun, & Ye, 2017; Xi et al., 2016; Xi, Fan, Wang, Liu, & Endo, 2015; Wang, Xi, Wan, Zhao, & Liu, 2014) have been made. Among these, the preparation of antimicrobial cotton textiles based on modification with silver nanoparticles (Ag NPs), offers one of the simplest processes which would fit with the capabilities of most finishing plants (Zhang, Xu, Fu, & Liu, 2016).

As an antimicrobial reagent, Ag NPs have desirable properties that include high specific surface area and high activity against a wide scope of pathogens. However, there have been concerns that Ag NPs may have health risks and environmental issues (Hernández-Arteaga et al., 2017). Previous work has indicated that the toxicity of Ag NPs is mainly caused by Ag ions leached from Ag NPs, and the toxicity strongly depends on the concentration of the leached ions (Parham et al., 2017). These issues are worrisome to the cotton textile industry, limiting the adoption of Ag NPs by scientists and engineers (Limpiteeprakan, Babel, Lohwacharin, & Takizawa, 2016; Shaheen & Fouda, 2014).

To enhance adhesion between Ag NPs and the cotton fiber surface, numerous strategies have been reported in the last decade (He, Xin, Chen, & Liu, 2018; Karim, Anderson, Singh, Ramanathan, & Bansal, 2018; Zhang, Li, Huang, Ren, & Huang, 2018; Zhang, Shu, Su, & Zhu, 2018). Among these methods, many have focused on the use of polymeric binders because they can combine various functional groups in one polymer chain to accomplish two tasks simultaneously: linking with cotton fabric and immobilizing the Ag NPs. For example, polydopamine (Li et al., 2018) and amino-terminated hyperbranched polymers (HBP-NH_2) (Zhang, Zhang, Morikawa, & Chen, 2014) were reported to be very effective for binding Ag NPs onto the cotton surface. However, Ag NPs have large specific surface areas and high surface energies. Thus, they favor aggregation to form larger nanoparticles during the coating process. Generally, larger Ag NPs are easier to wash off of the fiber surface. Therefore, for Ag NPs, both immobilization and control of the size and dispersion are important.

Chitosan has a several amine groups that can form coordination bonds with Ag NPs, but it cannot form covalent bonds with cotton fibers. Many methods, such as ones using plasma technology, cross-

* Corresponding authors.
E-mail addresses: diaohy@zju.edu.cn (H. Diao), liuxd@zstu.edu.cn (X. Liu).

https://doi.org/10.1016/j.carbpol.2018.09.089
Received 14 June 2018; Received in revised form 30 September 2018; Accepted 30 September 2018
Available online 03 October 2018
0144-8617/

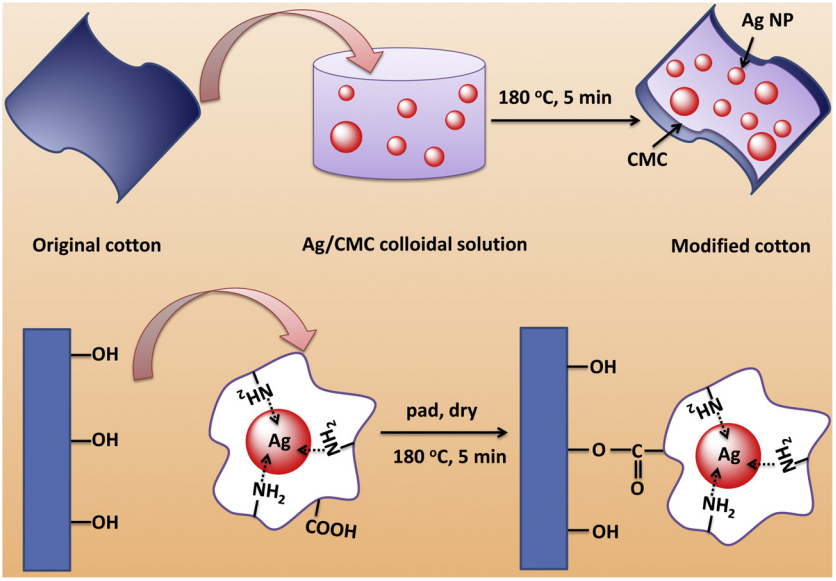

Scheme 1. The illustration of procedure to prepare the modified cotton fabrics.

linking techniques, and oxidation treatments, have been attempted (Dechojarassri et al., 2017; Liu, Nishi, Tokura, & Sakairi, 2001; Liu, Tokura, Nishi, & Sakairi, 2003) to link chitosan chains onto the cotton surface. Most of these treatments use toxic chemicals or complex processes.

In this study, a colloidal solution containing Ag NPs has been successfully prepared by using carboxymethyl chitosan (CMC) as a stabilizer. Because CMC has amine groups and carboxylic acid groups, it was expected to form coordination bonds with Ag NPs and to react with the hydroxyl groups of cellulose. Therefore, this modification could be carried out using a pad-dry-cure process (Dhineshbabu & Bercy, 2018; Ortelli et al., 2018).

In this effort, a colloidal solution of Ag NPs protected by CMC was first prepared and then used to immobilize the Ag NPs in a pad-dry-cure process within a few minutes. Notably, this one-pot method is operationally easy and could simplify the finishing process (Haraguchi, Hirai, Ozawa, Miyamoto, & Tanaka, 2012; Pedroza-Toscano et al., 2017). Fourier transform infrared (FTIR) spectroscopy, X-ray diffraction (XRD), X-ray photoelectron spectroscopy (XPS), and field emission scanning electron microscopy (FE-SEM) were used to characterize the modified cotton fabrics. Moreover, the antimicrobial activity and laundering durability of these modified cotton fabrics were evaluated by using an improved AATCC 100–1999 method.

2. Experimental

2.1. Materials

CMC (Mw, 15 kDa; deacetylation degree, > 95%; substitute degree, 80%) was purchased from Zhejiang Golden-Shell Pharmaceutical Co., Ltd (China). The cotton fabric was obtained from Shaoxing Qidong Textile Co., Ltd (60 ends/cm, 30 picks/cm, 0.42 mm thickness, 120 g/m weight, 35.2 m^2/g specific surface area). Before chemical modification, cotton fabric was cleaned as previous works (Xu, Gu, Zhao, Ke, & Liu, 2017; Xu, Wu, Zhang, Fu, & Liu, 2016; Xu, Xie et al., 2017). The human immortalized keratinocytes (Hacat) cells were purchased from iCell Bioscience Inc (Shanghai, China). The Dulbecco's modified Eagle's medium (DMEM), fetal bovine serum (FBS), and penicillin/streptomycin solution were purchased from Gibco (CA, USA). The Annexin V-FITC Apoptosis Detection Kit was purchased from BD Biosciences (San Diego, CA, USA). The cell counting kit-8 (CCK-8) was purchased from Dojindo (Japan). Before assay, the Hacat cells were cultured in DMEM, supplemented with 10% FBS, 100 U/mL penicillin and 100 μg/mL streptomycin at 37 °C, 5% CO_2. Other reagents were bought from Shanghai Aladdin Co., Ltd (China) and without further purification.

2.2. Preparation of Ag NPs/CMC colloidal solution and modification of cotton fabrics

CMC solution (1 wt %) was firstly prepared, mixed with an aqueous solution of $AgNO_3$ (10 mL, 0.47 mol/L) and $NaBH_4$ solution (10 mL, 0.94 mol/L), stirred at 25 °C for 30 min to obtain Ag NPs/CMC colloidal solution. A piece of cotton fabric (3.0 cm × 3.0 cm) was immersed in the colloidal solution, stirred at 25 °C for 30 min, padded to give a wet pick up of 80 ± 2% (by squeezing rollers), cured at 180 °C for 5 min, rinsed with distilled water (50 mL × 3 times), dried at 100 °C to obtain sample Cotton-1. The sample of Cotton-2 was prepared via a similar process but a 2 wt % CMC solution was used (Table S1).

2.3. Characterizations

Transmission electron microscopy (TEM; TF20, FEI, America) was used to study the size distribution of Ag NPs. The size distribution of the Ag NPs in the colloidal solution was statistically calculated by measuring 100 bright points in the TEM images using ImageJ software. The size distribution of the Ag NPs on fiber surface was statistically calculated by measuring 300 bright points in the SEM images. Other instruments such as FE-SEM, EDS, ATR, XRD, XPS, and ICP-MS were same to our previous reports (Xu, Gu et al., 2017; Xu, Xie, 2017; Xu, Ke, Cai et al., 2018; Xu, Ke, Shen et al., 2018). Antibacterial test and cytotoxicity analysis were described in the "Supporting Information". Other tests, such as laundering durability, water absorptivity, water vapor permeability and tensile strength tests were same to the previous work (Xu, Gu et al., 2017; Xu et al., 2016; Xu, Xie et al., 2017).

3. Results and discussion

3.1. Characterization of the Ag NPs/CMC colloidal solution and the modified cotton fabrics

Scheme 1 describes the one-pot modification process of the cotton fabric. A colloidal solution of Ag NPs stabilized by CMC was first prepared. As shown in Fig. 1, the TEM images show that the Ag NPs have spherical shapes. It is thought that the CMC chains would adsorb onto

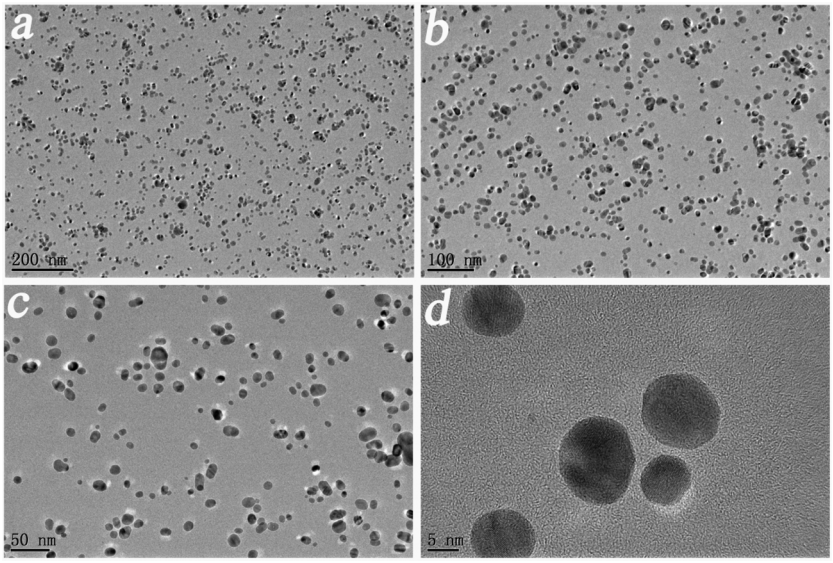

Fig. 1. TEM images of CMC/Ag NPs at various magnifications.

the surface of the Ag NPs via coordination bonds between the silver and the amine groups. The cotton fabric was then modified using the colloidal solution in a pad-dry-cure process. Two fabric samples are produced and labeled Cotton-1 and Cotton-2. A heating treatment, performed at 180 °C for 5 min induced esterification reactions between the carboxylic groups of CMC and the hydroxyl groups of the cotton fabrics (Qi, Huang et al., 2016; Qi, Zhao, Qing, Yan, & Sun, 2016).

Fig. S1a gives the size distribution of the Ag NPs, and the mean size of the Ag NPs was calculated as 18.1 ± 0.8 nm. The Ag NPs in the colloidal solution were studied by XRD technique, as shown in Fig. S1b. The peaks at 38°, 44°, 64° and 77° are assigned to the Ag (111), (200), (220), and (311) planes, respectively, meaning that the resulting Ag NPs have a pure and crystalline structure (Hasan, Waibhaw, Saxena, & Pandey, 2018; Zhang et al., 2017).

The ATR-FTIR spectra of the cotton fabrics are shown in the Fig. S2. The characteristic bands corresponding to cellulose appear at 1430 cm^{-1} (C—H wagging), 1364 cm^{-1} (C—H bending), 1105 cm^{-1} (C—O—C, asymmetric bridge stretching), 1160 cm^{-1}, 1060 cm^{-1} and 1028 cm^{-1} (C—O stretching). These bands are seen with both the original cotton and with the modified cotton fabrics, suggesting the chemical structure of the cellulose is mostly unchanged. In comparison with the original cotton fabric (Fig. S2a), the Cotton-1 (Fig. S2b) and Cotton-2 (Fig. S2c) fabrics show new peaks at 1545 cm^{-1} and 1732 cm^{-1}, which are assignable to NH_2 groups (N—H bending) (Zhang, Chen, Zang, Chen, & Lin, 2013), COOH groups and COOR groups (not carboxylate ions), respectively (Lv, Zhou, Liu, Gao, & Wang, 2014; Xu, Gu et al., 2017). These results suggest that esterification reactions have occurred between the CMC and the cotton fabric surfaces.

The XRD analyses were also performed on the modified cotton fabrics. As shown in Fig. 2, in comparison with original cotton fabric, typical peaks for the cellulose I crystalline form (Li et al., 2017) were observed at 2θ = 14.7°, 16.4°, 22.6°, and 34.3° in the XRD curves of Cotton-1 and Cotton-2 fabrics, suggesting that the cotton fibers have not been significantly damaged after the heating process for the deposition of the Ag NPs. Additionally, the characteristic peaks belonging to Ag NPs, which were observed from the colloidal solution (Fig. S1b), appear in the curves of the Cotton-1 and Cotton-2 fabrics. These results indicate that Ag NPs have been immobilized on the surface of the modified cotton fabrics, and their crystalline structure remains the same as that seen with the Ag NPs in the colloidal solution (Zhang, Li et al., 2018; Zhang, Shu et al., 2018). Based on the XRD spectra and the Debye–Scherrer equation (described in the "Supporting Information"),

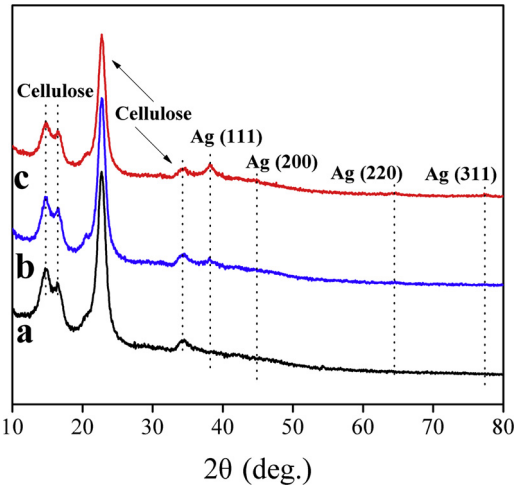

Fig. 2. XRD images of (a) original cotton, (b) Cotton-1, and (c) Cotton-2 fabric samples.

the average sizes of Ag NPs on the modified cotton fabrics, i.e., Cotton-1 and Cotton-2, were 41.5 nm and 63.9 nm, respectively. These results are greater than that of the Ag NPs dispersed in the colloidal solution (18.1 nm), meaning a certain degree of aggregation of the particles occurs during the coating process.

The wide-range XPS technique was used to study the modified cotton surface. As shown in Fig. 3a and b, comparison with the XPS spectrum of the original cotton fabric (has only C 1 s and O 1 s signals) shows additional N 1 s and Ag 3d signals in the XPS spectra of the Cotton-1 fabric. Further examination of the C1 s high resolution XPS spectra (Fig. 3c and d) was undertaken to analyze the coating structure on the surface of cotton fibers. The C1 s peak of the original cotton fabric shows three peaks at 284.1 eV (C—C), 286.2 eV (C—OH), and 288.7 eV (C—O—C). In the case of the Cotton-1 fabric, however, two new peaks appear at 285.7 eV and 288.8 eV. These are ascribed to C—N and C═O/C—O—C bonds, respectively (Xu, Gu et al., 2017; Xu, Xie, 2017). As shown in Fig. S3a, the peaks at 401.4 eV and 399.3 eV are attributable to the highly de-electronated N elements. Fig. S3b shows the Ag 3d spectra of the Cotton-1 and Cotton-2 fabrics. The binding energies of 374.2 eV and 368.1 eV are seen, corresponding to Ag 3d 5/2 and Ag 3d 3/2, respectively (Rehan, El-Naggar, Mashaly, & Wilken, 2018; Zou et al., 2013). These XPS results suggest that the amine groups

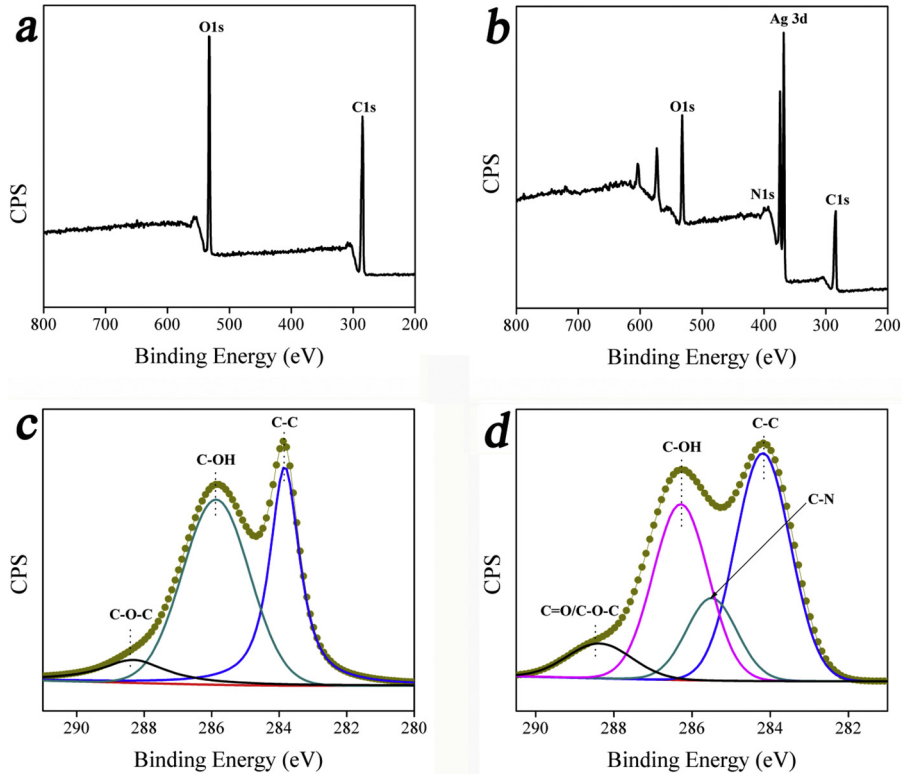

Fig. 3. XPS survey spectra and deconvoluted Cls XPS spectra of the original cotton (a, c) and the Cotton-1 (b, d) fabric samples.

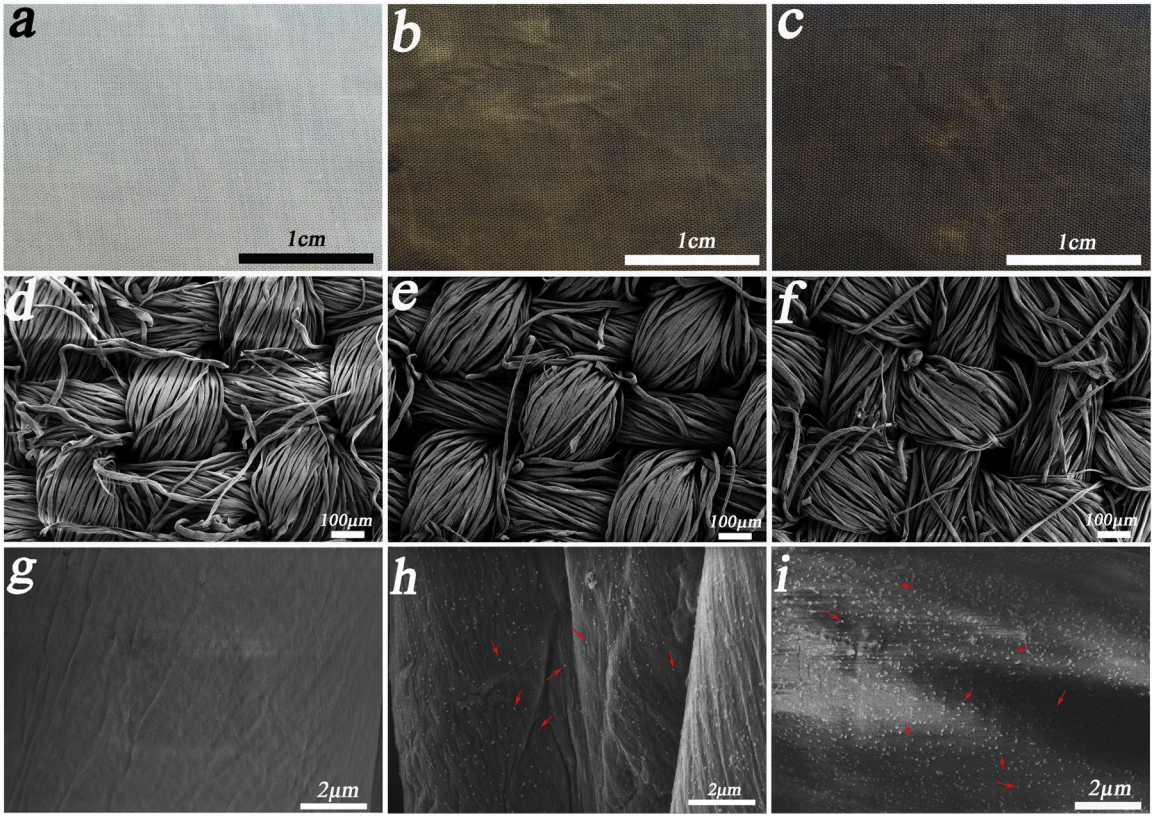

Fig. 4. The optical and SEM images of the original cotton (a, d, g), Cotton-1 (b, e, h), and Cotton-2 (c, f, i) fabric samples.

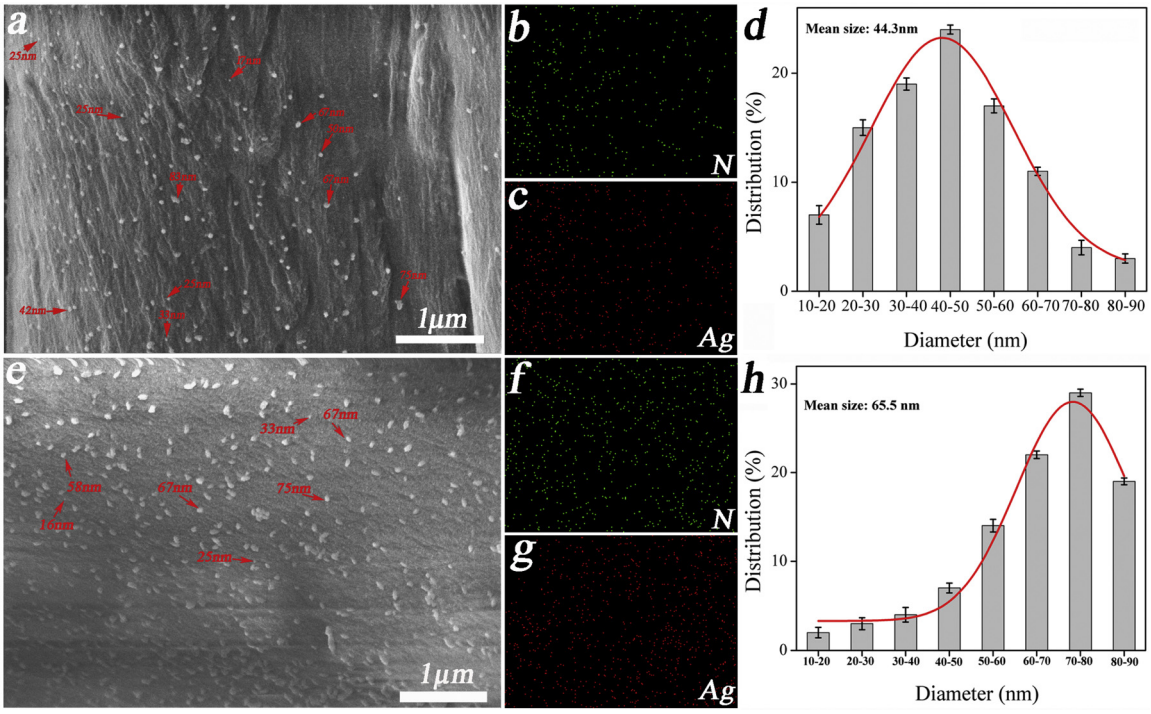

Fig. 5. High magnification (×20,000) SEM images, EDS mapping images, and size distribution of Cotton-1 (a–d) and Cotton-2 (e–h) fabric samples.

of CMC form coordination bonds with Ag NPs, and the CMC chain is grafted on the fiber surface via the linkage of ester groups.

The optical images and the different magnification SEM images of the cotton fabrics are shown in Fig. 4. In the optical images (Fig. 4a–c) of the cotton fabric samples, the color of the modified cotton fabric has darkened in comparison to the original cotton, indicating that the Ag NPs have been successfully loaded onto the cotton fabric surface. In the low-magnification SEM images (Fig. 4d–f), the change in the surface of the modified cotton fabrics is insignificant, implying that the Ag NPs mainly coat the cotton fiber surface and do not occupy the voids between the fibers. In the high-magnification SEM images (Fig. 4g–i), the original cotton fiber surface is clean and smooth, but numerous particles are observed on the fiber surfaces of the Cotton-1 and Cotton-2 fabrics.

The size and dispersion of the Ag NPs coating the surface of the modified cotton fabrics are confirmed by the high-magnification (×20,000) SEM images shown in Fig. 5a and e. The EDS mapping images (Fig. 5b, c, f and g) of the modified cotton fabric surfaces show the distribution of N and Ag. These images again confirm that the Ag NPs are immobilized on the cotton fabric surfaces. Statistical analysis of the bright points were performed, giving size distribution diagrams based on the high magnification (×20,000) SEM images. As shown in Fig. 5d and h, the Ag NPs on the modified cotton fabric samples, Cotton-1 and Cotton-2, have average sizes of 44.3 nm and 65.5 nm, respectively. This result is in good agreement with size data for Ag NPs which was calculated by the Debye-Scherrer equation based on the XRD images. Moreover, the SEM images again show that the Ag NPs are uniformly dispersed on the cotton fabric surface.

3.2. Antimicrobial effect and laundering durability

Antimicrobial tests were performed to investigate the antimicrobial behavior of the modified cotton fabrics. Fig. S4 shows the inhibition zones of the modified cotton fabrics, indicating that the antimicrobial effect against both *E. coli* and *S. aureus* are very effective when compared with the original cotton fabric. Fig. 6a and Table S1 show the antimicrobial effect of the modified cotton fabrics. The BR values of the modified cotton fabric (Cotton-1 and Cotton-2) for both bacteria after a 1 h contact period are both 100%. This indicates that the Ag NPs coating the cotton fabric provide excellent antibacterial properties.

The laundering durability is another important parameter for antimicrobial cotton fabrics. In this work, the modified cotton fabrics were subjected to washing tests, and the antibacterial performance was monitored after every ten laundering cycles. As shown in Fig. 6b and c, the antimicrobial rate of the Cotton-1 and Cotton-2 fabrics for both *E. coli* and *S. aureus* remained over 94% and 96%, even after 50 washing cycles, respectively.

To examine the quality of Ag NPs on the cotton fabric surface, elemental analyses of the cotton fabrics before and after laundering cycles were carried out using an ICP-MS technique. As shown in Table S2, the loss of Ag NPs is significant in the first 30 cycles. After that, the amount of Ag NPs on the cotton remains steady with subsequent washing cycles. After 50 laundering tests, about 84.8% of the Ag NPs remained on the cotton surface in comparison to cotton fabrics that had not been washed. The results reveal again that the pad-dry process using the Ag/CMC colloidal solution provides a modified cotton fabric with a remarkable durability to laundering.

Fig. S5 compares the SEM images, EDS mapping images, and the size distribution of the modified cotton fabric samples (Cotton-1 and Cotton-2 fabric samples) after 50 washing tests. Similar to the fabric before washing, the EDS mapping images demonstrate that the bright points in the SEM images are Ag NPs. It was found that the Ag NPs on the modified cotton fabric samples, Cotton-1 and Cotton-2, have average sizes of 35.0 nm and 44.2 nm, respectively. These results confirm again that most of the Ag NPs still exist on the washed cotton fiber surface, even after 50 washing cycles. However, the size of the Ag NPs becomes smaller when comparing the washed samples with those that have not been laundered. During the washing process, larger Ag NPs are more rapidly washed off than the smaller Ag NPs. Additionally, ionic leaching from Ag NPs may also lead to their size reduction.

To evaluate the toxicity caused by the Ag NPs on the cotton fabrics, cytotoxicity tests using Human immortalized keratinocytes (Hacat) were carried out by exposing the cells to the leachate solutions (Table S3). The apoptosis of Hacat cells was evaluated by flow cytometry via

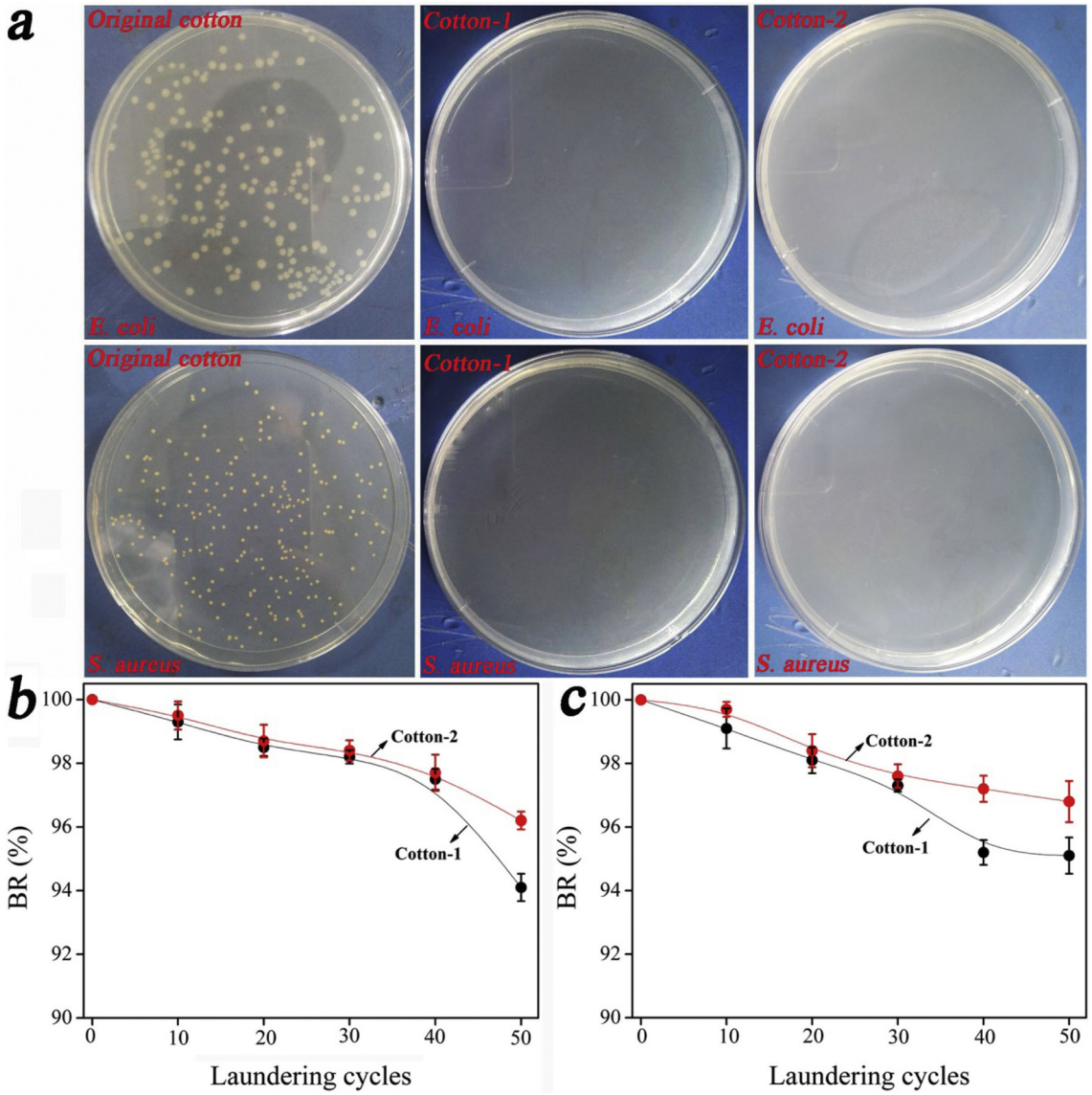

Fig. 6. The antibacterial effect of the cotton fabric samples, the optical images of the antibacterial tests (a), and the durability results of the antibacterial properties against *E. coli* (b) and *S. aureus* (c).

double staining with Annexin V-FITC and propidium iodide (PI). As shown in Fig. 7(1), the three samples show a similar percentage of apoptosis cells (Annexin V^+/PI– and Annexin V^+/PI^+ cells), and they are not obviously different from the results for the physiological saline solution (control). The microscopy images of the incubated Hacat cells are shown in Fig. 7(2). These show no significant changes in the morphology and quantity of the Hacat cells. The in vitro cytotoxicity of the leachate solutions against Hacat cells was examined by a CCK-8 assay. As shown in Fig. 7(3), the results indicate that the leachate solutions have no cytotoxicity for Hacat cells. These results are in good agreement with a previous report (Rehan et al., 2018), and reveal that the modified cotton fabric is safe for human skin.

3.3. Influences on the intrinsic nature of cotton

Considering that the modified cotton fabrics should be comfortable to the human skin, the nature of cotton fabric such as its vapor permeability and water absorbability should be reserved in the modifications process (Xu, Ke, Ge et al., 2018). Therefore, these two properties were tested in this work.

As shown in the Fig. 8(1) and (2), the modified cotton fabric shows slightly lower vapor permeability when compared with the original cotton fabric (vapor permeability of 1147 ± 12 $g/m^2/d$). Moreover, the vapor permeability of the Cotton-1 fabric is better than that of the Cotton-2 fabric. This is attributable to blockage of the gaps between the cotton fibers by CMC. However, as CMC is hydrophilic, water absorbability of the modified cotton fabrics is better than that of the original fabric (water absorbability of 272.0 ± 4.2%). The mechanical properties (Fig. 8(3)) of the cotton fabrics were also studied by measuring the breaking tensile strength. The tensile breaking strength for the modified cotton is almost equal to that of the original cotton. Fig. 8(4) compares the flexibilities of the original cotton and the Cotton-1 sample. The original cotton fabric has good flexibility with the height of the loop being at 10.9 mm. The Cotton-1 fabric showed a small loop height of 13.0 mm, which is slightly higher than that seen with the original cotton fabric.

4. Conclusions

A CMC/Ag NP colloidal solution was used to modify cotton fabrics via a simple pad-dry-cure process. The modified cotton fabric has good antibacterial properties and gives a 100% BR rate against both *S. aureus*

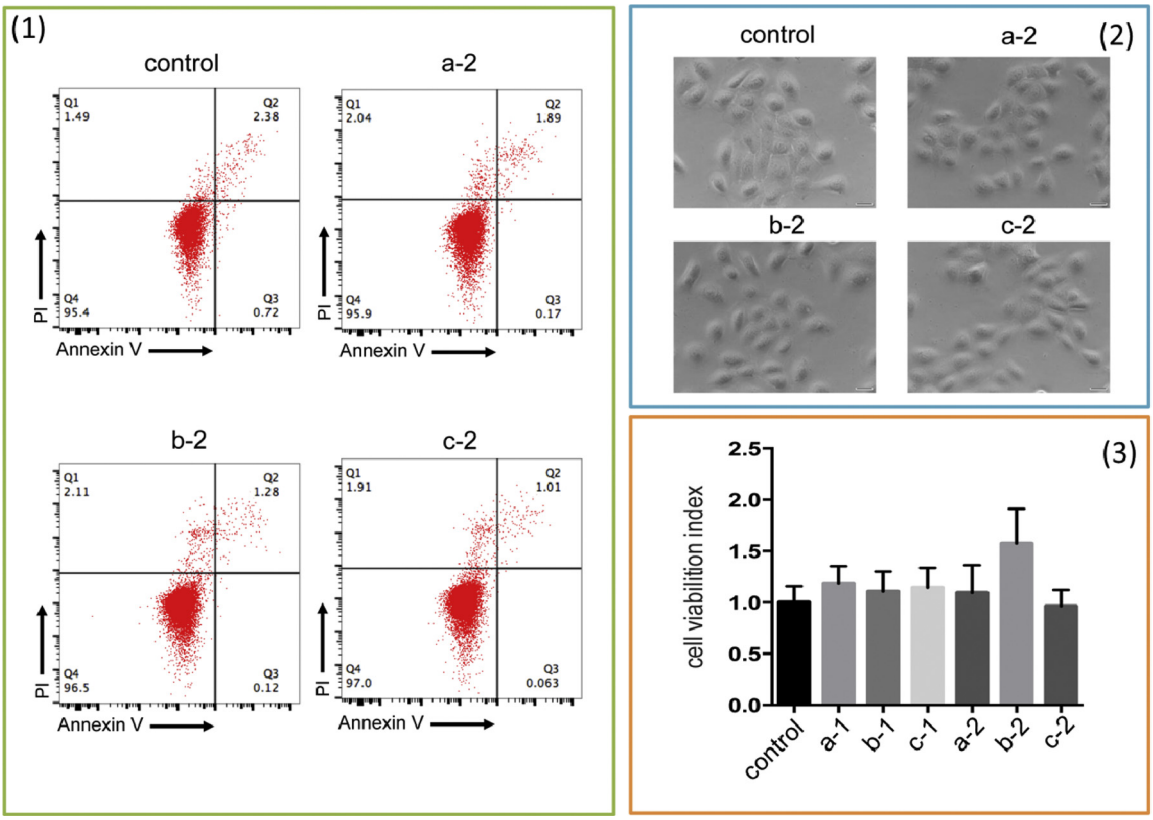

Fig. 7. Toxicity test results of the leachate solutions obtained from cotton fabric containing Ag NPs. (1) Induction of apoptosis assessed with flow cytometry analysis of annexin V and propidium iodide (PI) staining of the cells. (2) Representative microscopic images of the incubated Hacat cells. (3) In vitro cytotoxicity (CCK-8) of the leachate solutions. Data are presented as the mean ± SD (n = 5), (The leachate was obtained by incubating the original cotton fabric for 24 h (a), the Cotton-1 fabric for 12 h (b), and the Cotton-1 fabric for 24 h (c) in physiological saline solution).

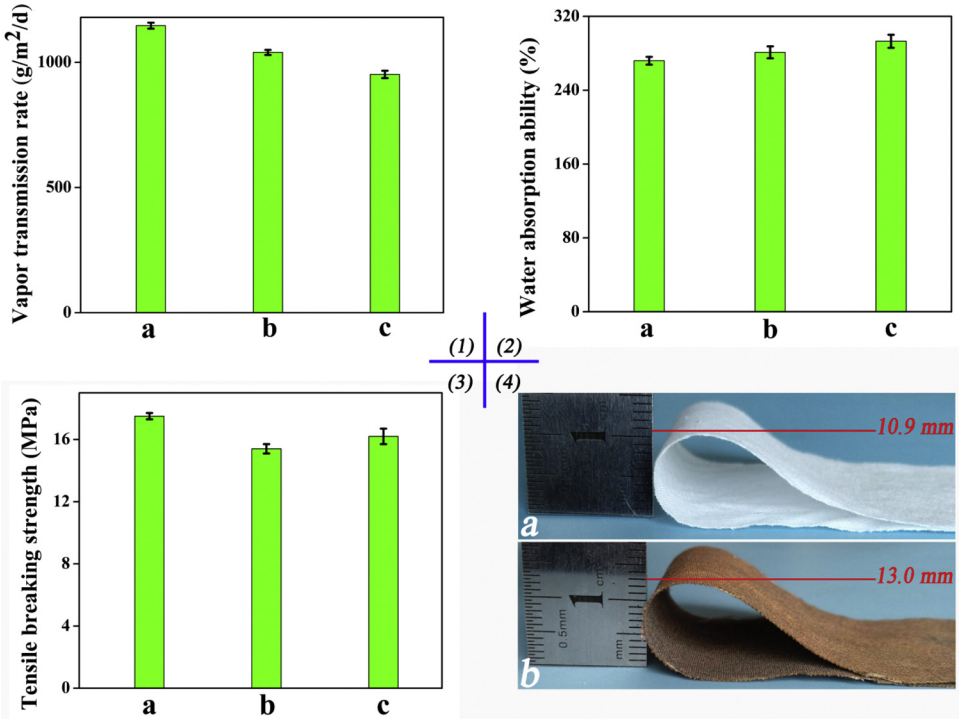

Fig. 8. Influence of the surface modification on the nature of cotton, including (1) water vapor transmissibility, (2) water absorbability, (3) tensile strength, and (4) flexibility. (a) Original cotton, (b) Cotton-1, and (c) Cotton-2 fabric samples.

and *E. coli*. Even after 50 washing cycles, the content of silver on the modified cotton fabric decreases to only 84.8% that of its original value, and the BR rates against both *S. aureus* and *E. coli* remain above 94%. Importantly, the modification process does not significantly affect the inherent attractive attributes of cotton fabric.

Acknowledgement

This work was financially supported by Public Welfare Technology Application Research Project of Zhejiang Province (2017C31035) and the Natural Science Foundation of China (51573167).

Appendix A. Supplementary data

Supplementary material related to this article can be found, in the online version, at doi:https://doi.org/10.1016/j.carbpol.2018.09.089.

References

Dechojarassri, D., Asaina, S., Omote, S., Nishida, K., Furuike, T., & Tamura, H. (2017). Adsorption and desorption behaviors of cesium on rayon fibers coated with chitosan immobilized with Prussian blue. *International Journal of Biological Macromolecules, 104*, 1509–1516.

Dhineshbabu, N. R., & Bercy, E. W. (2018). Multifunctional property of graphene oxide nanostructures on silica-coated cotton fabrics. *Journal of Nanoscience and Nanotechnology, 18*, 4923–4929.

Fei, Z., Liu, B., Zhu, M., Wang, W., & Yu, D. (2018). Antibacterial finishing of cotton fabrics based on thiol-maleimide click chemistry. *Cellulose, 25*, 3179–3188.

Feng, J., Sun, M., & Ye, Y. (2017). Ultradurable underwater superoleophobic surfaces obtained by vapor-synthesized layered polymer nanocoatings for highly efficient oil–water separation. *Journal of Materials Chemistry A, 5*, 14990–14995.

Haraguchi, M., Hirai, T., Ozawa, M., Miyamoto, M., & Tanaka, K. (2012). One-step synthesis of hyper-branched polymer with perfluoroalkyl segments. *KGK Kautschuk Gummi Kunststoffe, 65*, 34–38.

Hasan, A., Waibhaw, G., Saxena, V., & Pandey, L. M. (2018). Nano-biocomposite scaffolds of chitosan, carboxymethyl cellulose and silver nanoparticle modified cellulose nanowhiskers for bone tissue engineering applications. *International Journal of Biological Macromolecules, 111*, 923–934.

He, S., Xin, B., Chen, Z., & Liu, Y. (2018). Flexible and highly conductive Ag/G-coated cotton fabric based on graphene dipping and silver magnetron sputtering. *Cellulose, 25*, 3691–3701.

Hernández-Arteaga, A., Nava, J. D. J. Z., Kolosovas-Machuca, E. S., Velázquez-Salazar, J. J., Vinogradova, E., José-Yacamán, M., et al. (2017). Diagnosis of breast cancer by analysis of sialic acid concentrations in human saliva by surface-enhanced Raman spectroscopy of silver nanoparticles. *Nano Research, 10*, 3662–3670.

Hu, J., Gao, Q., Xu, L., Wang, M., Zhang, M., Zhang, K., et al. (2018). Functionalization of cotton fabrics with highly durable polysiloxane–TiO_2 hybrid layers: Potential applications for photo-induced water–Oil separation, UV shielding, and self-cleaning. *Journal of Materials Chemistry A, 6*, 6085–6095.

Karim, M. N., Anderson, S. R., Singh, S., Ramanathan, R., & Bansal, V. (2018). Nanostructured silver fabric as a free-standing NanoZyme for colorimetric detection of glucose in urine. *Biosensors and Bioelectronics, 110*, 8–15.

Li, Y., Wang, B., Sui, X., Xie, R., Xu, H., Zhang, L., et al. (2018). Durable flame retardant and antibacterial finishing on cotton fabrics with cyclotriphosphazene/polydopamine/silver nanoparticles hybrid coatings. *Applied Surface Science, 435*, 1337–1343.

Li, Z., Meng, J., Wang, W., Wang, Z., Li, M., Chen, T., et al. (2017). The room temperature electron reduction for the preparation of silver nanoparticles on cotton with high antimicrobial activity. *Carbohydrate Polymers, 161*, 270–276.

Limpiteeprakan, P., Babel, S., Lohwacharin, J., & Takizawa, S. (2016). Release of silver nanoparticles from fabrics during the course of sequential washing. *Environmental Science and Pollution Research, 23*, 22810–22818.

Liu, X. D., Nishi, N., Tokura, S., & Sakairi, N. (2001). Chitosan coated cotton fiber: Preparation and physical properties. *Carbohydrate Polymers, 44*, 233–238.

Liu, X. D., Tokura, S., Nishi, N., & Sakairi, N. (2003). A novel method for immobilization of chitosan onto nonporous glass beads through a 1, 3-thiazolidine linker. *Polymer, 44*, 1021–1026.

Lv, J., Zhou, Q., Liu, G., Gao, D., & Wang, C. (2014). Preparation and properties of polyester fabrics grafted with O-carboxymethyl chitosan. *Carbohydrate Polymers, 113*, 344–352.

Ortelli, S., Malucelli, G., Cuttica, F., Blosi, M., Zanoni, I., & Costa, A. L. (2018). Coatings made of proteins adsorbed on TiO_2 nanoparticles: A new flame retardant approach for cotton fabrics. *Cellulose, 25*, 2755–2765.

Parham, S., Nemati, M., Sadir, S., Bagherbaigi, S., Wicaksono, D. H., & Nur, H. (2017). In situ synthesis of silver nanoparticles for AgNP/cotton nanocomposite and its bactericidal effect. *Journal of the Chinese Chemical Society, 64*, 1286–1293.

Pedroza-Toscano, M. A., López-Cuenca, S., Rabelero-Velasco, M., Moreno-Medrano, E. D., Mendizabal-Ruiz, A. P., & Salazar-Peña, R. (2017). Silver nanoparticles obtained by semicontinuous chemical reduction using carboxymethyl cellulose as a stabilizing agent and its antibacterial capacity. *Journal of Nanomaterials*(2017).

Qi, H., Huang, Y., Ji, B., Sun, G., Qing, F. L., Hu, C., et al. (2016). Anti-crease finishing of cotton fabrics based on crosslinking of cellulose with acryloyl malic acid. *Carbohydrate Polymers, 135*, 86–93.

Qi, H., Zhao, C., Qing, F. L., Yan, K., & Sun, G. (2016). Antiwrinkle finishing of cotton fabrics with 5-(Carbonyloxy succinic)-benzene-1, 2, 4-tricarboxylic acid: Comparison with other acids. *Industrial & Engineering Chemistry Research, 55*, 11850–11856.

Rauytanapanit, M., Opitakorn, A., Terashima, M., Waditee-Sirisattha, R., & Praneenararat, T. (2018). Antibacterial cotton fabrics based on hydrophilic amino-containing scaffolds. *Colloids and Surfaces B: Biointerfaces, 164*, 42–49.

Rehan, M., El-Naggar, M. E., Mashaly, H. M., & Wilken, R. (2018). Nanocomposites based on chitosan/silver/clay for durable multi-functional properties of cotton fabrics. *Carbohydrate Polymers, 182*, 29–41.

Ren, G., Song, Y., Li, X., Wang, B., Zhou, Y., Wang, Y., et al. (2018). A simple way to an ultra-robust superhydrophobic fabric with mechanical stability, UV durability, and UV shielding property. *Journal of Colloid and Interface Science, 522*, 57–62.

Salat, M., Petkova, P., Hoyo, J., Perelshtein, I., Gedanken, A., & Tzanov, T. (2018). Durable antimicrobial cotton textiles coated sonochemically with ZnO nanoparticles embedded in an in-situ enzymatically generated bioadhesive. *Carbohydrate Polymers, 189*, 198–203.

Shaheen, T. I., & Fouda, A. (2014). Green approach for one-pot synthesis of silver nanorod using cellulose nanocrystal and their cytotoxicity and antibacterial assessment. *International Journal of Biological Macromolecules, 106*, 784–792.

Wang, L., Xi, G. H., Wan, S. J., Zhao, C. H., & Liu, X. D. (2014). Asymmetrically superhydrophobic cotton fabrics fabricated by mist polymerization of lauryl methacrylate. *Cellulose, 21*, 2983–2994.

Xi, G., Fan, W., Wang, L., Liu, X., & Endo, T. (2015). Fabrication of asymmetrically superhydrophobic cotton fabrics via mist copolymerization of 2, 2, 2-trifluoroethyl methacrylate. *Journal of Polymer Science Part A: Polymer Chemistry, 53*, 1862–1871.

Xi, G., Wang, J., Luo, G., Zhu, Y., Fan, W., Huang, M., et al. (2016). Healable superhydrophobicity of novel cotton fabrics modified via one-pot mist copolymerization. *Cellulose, 23*, 915–927.

Xu, Q., Wu, Y., Zhang, Y., Fu, F., & Liu, X. (2016). Durable antibacterial cotton modified by silver nanoparticles and chitosan derivative binder. *Fibers and Polymers, 17*, 1782–1789.

Xu, Q., Gu, J., Zhao, Y., Ke, X., & Liu, X. (2017). Antibacterial cotton fabric with enhanced durability prepared using L-cysteine and silver nanoparticles. *Fibers and Polymers, 18*, 2204–2211.

Xu, Q., Ke, X., Cai, D., Zhang, Y., Fu, F., Endo, T., et al. (2018). Silver-based, single-sided antibacterial cotton fabrics with improved durability via an l-cysteine binding effect. *Cellulose, 25*, 2129–2141.

Xu, Q., Ke, X., Ge, N., Shen, L., Zhang, Y., Fu, F., et al. (2018). Preparation of copper nanoparticles coated cotton fabrics with durable antibacterial properties. *Fibers and Polymers, 19*, 1004–1013.

Xu, Q., Ke, X., Shen, L., Ge, N., Zhang, Y., Fu, F., et al. (2018). Surface modification by carboxymethy chitosan via pad-dry-cure method for binding Ag NPs onto cotton fabric. *International Journal of Biological Macromolecules, 111*, 796–803.

Xu, Q., Xie, L., Diao, H., Li, F., Zhang, Y., Fu, F., et al. (2017). Antibacterial cotton fabric with enhanced durability prepared using silver nanoparticles and carboxymethyl chitosan. *Carbohydrate Polymers, 177*, 187–193.

Yang, Z., Zhang, Y., Fu, F., & Liu, X. (2017). Single-faced flame resistance of cotton fabrics modified via mist copolymerization. *RSC Advances, 7*, 53871–53877.

Zhang, D., Chen, L., Zang, C., Chen, Y., & Lin, H. (2013). Antibacterial cotton fabric grafted with silver nanoparticles and its excellent laundering durability. *Carbohydrate Polymers, 92*, 2088–2094.

Zhang, M., Pang, J., Bao, W., Zhang, W., Gao, H., Wang, C., et al. (2017). Antimicrobial cotton textiles with robust superhydrophobicity via plasma for oily water separation. *Applied Surface Science, 419*, 16–23.

Zhang, Y., Xu, Q., Fu, F., & Liu, X. (2016). Durable antimicrobial cotton textiles modified with inorganic nanoparticles. *Cellulose, 23*, 2791–2808.

Zhang, G., Zhang, F., Morikawa, H., & Chen, Y. (2014). One-step synthesis of silver nanoparticles in an aqueous solution and their antibacterial activities. *Applied Physics A, 114*, 1277–1283.

Zhang, S., Li, R., Huang, D., Ren, X., & Huang, T. S. (2018). Antibacterial modification of PET with quaternary ammonium salt and silver particles via electron-beam irradiation. *Materials Science and Engineering: C, 85*, 123–129.

Zhang, X., Shu, Y., Su, S., & Zhu, J. (2018). One-step coagulation to construct durable anti-fouling and antibacterial cellulose film exploiting Ag@ AgCl nanoparticle-triggered photo-catalytic degradation. *Carbohydrate Polymers, 181*, 499–505.

Zou, M., Du, M., Zhu, H., Xu, C., Li, N., & Fu, Y. (2013). Synthesis of silver nanoparticles in electrospun polyacrylonitrile nanofibers using tea polyphenols as the reductant. *Polymer Engineering & Science, 53*, 1099–1108.